AN EXPERIMENTAL STUDY OF THE EFFECTS OF DISK ROUGHNESS ON THE FLYING CHARACTERISTICS OF NEAR-CONTACT SLIDERS

Lei Yan and D. B. Bogy
Computer Mechanics Laboratory
Department of Mechanical Engineering
University of California, Berkeley

Abstract

In this experimental study, three disks with different roughnesses and three types of 50% sliders i. e. an AAB, the CML "nutcracker" and a Tripad were used to investigate the disk roughness effects on the flying characteristics, especially pitch and roll angles.

All three sliders exhibited higher pitch angle on the smoother disk than on the rougher disk. But the roll angle was not sensitive to the disk roughness.

On the rougher disk, the acoustic emission signal is higher, consistent with the lower spacing results, since the probability of random contact with the peaks of the disk is higher.

1. Introduction

Magnetic hard disk recording is used to store and retrieve information. Its information storage capacity is determined by the density of binary data bits stored per unit area on the disk. Hard disk drive (HDD) technology continues to experience a dramatic yearly increase in areal density of 60%. In order to get higher areal density, which is one of the main concerns of research and development of the hard disk industry, every component, including the disk, spindle and motor, slider suspension and head gimbal assembly, of the hard disk drive must have improved performance.

One of the most important improvements is the reduction of the spacing between the read write head and the disk, namely the flying height. Today's highest technology drive has MR read heads and flies at 59 nm (2-3 micro-inches). Sliders designed to have substantial contact with the disk during operation but with almost all of the suspension load supported by the air bearing are called proximity sliders. Decreasing the flying height increases the potential for contact between the slider and the disk. In this interface, the disk's morphology, roughness and waviness, has important effects on the slider's flying characteristics.

Previous experimental research by Donovan et al. [1] discussed the disk surface roughness effects on the air- bearing in reference to a "guppy" slider and "nutcracker" slider. Bedoy et al.[2] studied the disk roughness effects on the landing curve slope in reference to the Tri-pad slider. Bair et al. [3] examined the disk waviness effects on proximity air bearing sliders. The principle motivation of these studies was to obtain a

better understanding of the slider's landing characteristics (near-contact/low velocity regime).

The purpose of this study is to investigate the disk roughness effects on the landing characteristics especially pitch and roll angles using proximity air bearing sliders and "super smooth" disks.

2. Measurement systems

2.1 Phase Metrics DFHT

The absolute spacing between the air bearing surface and a glass disk can be measured using white light interferometry. When a white light measurement beam is directed through a glass disk the light is reflected off the air bearing surface and the adjacent surface of the glass disk. By measuring the light intensity and phase shift in the interference pattern the distance between them can be determined.

One instrument that uses white light interferometry is the Phase Metrics Dynamic Flying Height Tester (DFHT). It utilizes three wavelength interferometry (blue - 436 nanometer, green - 546 nanometer, yellow - 580 nanometer). The coherence length of the light is short in order to eliminate interference with light reflected from other surfaces e. g. the bottom surface of the glass disk. A unique value for the spacing is determined by comparing the measured light intensity and a set of theoretical spacing/intensity curves for the three wavelengths, also taking into account the complex coefficients of refraction (N and K values) (see Figures 2.1 and 2.2). The spacing can be measured in the range from 1016 nanometers down to near contact. The maximum sampling rate is 234.8 kHz.

The main drawback of DFHT is that it can only measure the spacing between a glass disk and the slider. This means it can not be used to investigate the actual disk surface effects on the air bearing.

2.2 The Polytec LDV

Frequency demodulation is utilized to measure the motion of one measurement spot or the relative motion between two targets. The Polytec LDV uses frequency demodulation. The linearly polarized light is split into two beams. An acousto-optic modulator is used in the path of one beam to generate the heterodyne frequency. After passing through various optical elements, the two beams are combined and the resulting interference is measured by two photo diodes. The Polytec LDV is relatively easy to operate, and it can measure velocity variation as well as spacing variation. Therefore it is very useful in vibration studies. However its highest DC resolution is only about 8 nm, which is not enough to be used in the spacing variation measurement.

2.3 The computer mechanics laboratory MCLI system

The MCLI (Multi-Channel Laser Interferometer) is a version of a heterodyne interferometer for measuring slider/disk spacing dynamics that was developed in CML (refs. [8], [9]). Figure 2.3 shows a schematic diagram of the MCLI. A laser beam (He-Ne, 632.8 nanometer) is split into two beams by an AOM. One is shifted up by 40 MHz and is used as the reference beam. The other beam, the measurement beam, passes through

the AOM and polarizing beam splitter (PBS) and is directed to the slider and the disk. Part of it is reflected off the back surface of the slider and part of it is reflected off the disk. The reflected beam is brought into interference with the reference beam. The interference pattern is captured by fiber optic probes and directed to photodiodes. The signals from the photodetectors are then analyzed in a phase demodulator. Then the spacing variation can be determined. The resolution of the MCLI electronics is 2.5 nm.

The main drawback of MCLI is that it only utilizes one measurement beam (see Figure 2.4). Because of this, the back surface of the slider has to be parallel to the surface of the disk within less than 0.1°. Not all standard sliders fulfill this requirement. The MCLI is no longer used in CML.

2.4 The BALI system

The BALI (Berkeley Axiom Laser Interferometer) system was developed in CML (refs. [1]). It utilizes two independent measurement beams and one reference beam. The optical setup is three dimensional (see Figure 2.5). Initially, a He-Ne laser beam is split into reference and measurement beams. After passing through optics elements, the measurement beam is directed on the target. Then, the reflection signal combines with the reference beam and interference occurs.

The interference pattern is coupled in two fiber probes. Two avalanche photo diodes detect the intensity of the light. When measuring relative flying height changes, the target points include the back surface of the slider and a point on the disk. By using the

ZYGO Axiom 2/20 interferometer system to take the phase difference between the two selected points, the relative spacing is determined.

The maximum sampling rate of BALI is 180kHz and its resolution is 2.5 nm.

2.5 The "box"

Utilizing the same optical setup as BALI, a new phase demodulator was built in CML(refs [10]). The new phase demodulator directly measures the relative spacing between two targets. It reduces the number of operations and so decreases the noise level of the measurements.

In this research, the relative spacing is measured at constant linear velocity. For every experiment , the average value (DC offset) of the signal is measured (Figure 2.6). By changing the rotational speed, the relationship between flying height and linear velocity is obtained.

2.6 AE sensor

AE measurement techniques have been widely used in head-disk interface analysis.

In general, an AE is defined as a transient elastic wave generated by a rapid spontaneous release of energy when materials undergo deformation and/or fracture. An AE sensor is a device which generates an electrical signal when it is stimulated by an acoustic wave.

In this research, acoustic emission is detected by mounting a piezoeletric transducer (PZT) near the base of the suspension. The RMS value of acoustic emission can be used to determine whether or not the slider contacts with the disk.

2.7 The ZYGO New View 100

The ZYGO New View 100 is a general purpose, three dimensional, imaging surface structure analyzer (refs [6]). It uses coherence scanning white light interferometry to image and measure the micro structure and topography of surfaces in three dimension without contacting the surface. Light from the microscope divides, one portion reflects from the test surface and another portion reflects from an internal high quality reference surface. Both portions are then directed onto a solid state camera. The test part is scanned by vertically moving the objective with a PZT. As the objective scans, a video system captures intensities at each camera pixel. These intensities are converted into image by MetroPro software.

The ZYGO New View 100 analyzes and quantifies the surface topography of a part. Depths up to 100 micrometers with 0.1 nanometer resolution and 0.3 nanometer RMS repeatability are imaged independent of objective magnification.

3. Materials

3.1 Sliders

For these experiments, three proximity air bearing sliders were used. The air bearing designs were an AAB, the CML "Nutcracker" and a tripad. All were 50% sliders of length 2.0 millimeters and width 1.6 millimeters.

3.2 Suspensions

All sliders were mounted on gimbal style medium length (18 milimeters) suspension arms. The AAB was mounted on a 1950 type suspension with specified z-height of 27 miliinches. The CML " Nutcracker" slider was mounted on a 1950 type suspension which required a 23 miliinches z-height. The tripad slider was mounted on a 850 type suspension whose z-height was 29 miliinches.

3.3 Disks

Three disks were used. The substrates were NiP on which were deposited an under layer, a magnetic layer, an h:C overcoat and Z-dol lube. One of them had no applied additional texture. The other two were textured with a cross-hatched pattern along the circumferential direction.

4 Results and discussion

4.1 Disk roughness calibration

Disk surface roughness was examined by the Zygo NewView 100 using the 40X magnification objective. The reported results are the average of three measurements at a radius of 30mm. The results for the 5 Angstrom, 10 Angstrom and 15 Angstrom disks were 4.62, 8.91, 14.16 Angstroms respectively.

Plots of the untextured disk did not show any pattern in Figure 4.1, while the circumferential textures were clearly shown for the 10 Angstrom and 15 Angstrom disks in Figures 4.2 and 4.3

4.2 Relative spacing measurements

The BALI system measures relative spacing changes between the slider and disk, i.e. the spacing between the back surface of the slider and the disk. Using the BALI system and "the box", the relative flying height versus velocity can be determined as mentioned before. By putting one target point on the different corners of the slider, the relative spacing variation between the outer trailing (OT), inner trailing (IT) and inner leading (IL) corners of the slider and the disk can be measured.

Figures 4.4-4.6 show the OT, IT, IL landing curves of the AAB slider over three disks, respectively. In the 15 Angstrom disk case the relative spacing varied from 325 nm to 39

nm for IL, from 26 nm to 4 nm for IT and from 41 nm to 11 nm for OT as the velocity decreased. In the 10 Angstrom disk case the relative spacing varied from 403 nm to 45 nm for IL, from 25 nm to 4 nm for IT and from 46 nm to 9 nm for OT as the velocity decreased. In the 5 Angstrom disk case the relative spacing varied from 445 nm to 49 nm for IL, from 25 nm to 3 nm for IT and from 46 nm to 11 nm for OT as the velocity decreased.

Figures 4.7-4.9 show the OT, IT, IL landing curves of the Nutcracker slider over the three disks, respectively. In the 15 Angstrom disk case the relative spacing varied from 515 nm to 41 nm for IL, from 45 nm to 23 nm for IT and from 58 nm to 25 nm for OT as the velocity decreased. In the 10 Angstrom disk case the relative spacing varied from 545 nm to 43 nm for IL, from 45 nm to 23 nm for IT and from 59 nm to 27 nm for OT as the velocity decreased. In the 5 Angstrom disk case the relative spacing varied from 584 nm to 50 nm for IL, from 44 nm to 22 nm for IT and from 58 nm to 30 nm for OT as the velocity decreased.

Figures 4.10-4.12 show the OT, IT, IL landing curves of the Tripad slider over the three disks, respectively. In the 15 Angstrom disk case the relative spacing varied from 375 nm to 15 nm for IL, from 26 nm to 3 nm for IT and from 41 nm to 6 nm for OT as the velocity decreased. In the 10 Angstrom disk case the relative spacing varied from 466 nm to 19 nm for IL, from 23 nm to 3 nm for IT and from 40 nm to 10 nm for OT as the velocity decreased. In the 5 Angstrom disk case the relative spacing varied from 575 nm to 28 nm for IL, from 22 nm to 2 nm for IT and from 36 nm to 13 nm for OT as the velocity decreased.

On the smoother disk, the slider flying height is larger than it is over the rougher disk. the same trend is found in all three types of sliders.

4.3 Pitch and roll angle measurements

By taking the relative spacing difference between IT and IL, and then divided by 2mm, the pitch angles of the slider can be determined. By taking the relative spacing difference between IT and OT, and then divided by 1.6mm, the roll angles of the slider can be determined.

Figures 4.10, 4.12 and 4.14 show the pitch angles of the AAB, Nutcracker and tripad sliders over the three disks. The pitch angles of the AAB slider increased from 23 μrad to 215 μrad , 21 μrad to 189 μrad and 18 μrad to 150 μrad as the velocity increased for the 5 Angstrom, 10 Angstrom and 15 Angstrom disk, respectively. The pitch angles of the "Nutcracker" slider increased from 14 μrad to 270 μrad , 10 μrad to 250 μrad and 9 μrad to 235 μrad as the velocity increased for the 5 Angstrom, 10 Angstrom and 15 Angstrom disk, respectively. The pitch angles of the Tripad slider increased from 13 μrad to 276 μrad , 4 μrad to 213 μrad and 6 μrad to 176 μrad as the velocity increased for the 5 Angstrom, the 10 Angstrom and the 15 Angstrom disk, respectively.

Figures 4.11, 4.13 and 4.15 show the roll angles of the AAB, Nutcracker and Tripad slider over the three disks. The roll angles varied between 20 μrad and 5 μrad for all three sliders on the different disks.

4.4 Acoustic Emission results

A glider avalanche test was carried out for each slider over each disk by decreasing the rotational speed of the disk. All results were averaged over five measurements. Figures 4.16-4.18 show plots of the glide avalanche results for the AAB, Nutcracker and Tripad sliders over the 5, 10 and 15 Angstrom disks, respectively. For all three sliders, the AE RMS output increased as the disk velocity increased. Also the AE RMS had higher values on the rougher disks.

5 Discussions and Conclusions

On a smoother disk, the relative spacing between the inner leading (IL) corners of the slider and the disk is higher than it is on a rougher disk. The same trend was found for all three types of sliders. While the relative spacing between trailing edge of the slider and the disk does not show much difference on three different types of disks. Therefore all three sliders also exhibited higher pitch angles on the smoother disk. But the roll angle was not sensitive to the disk roughness. The change of the pitch angle is thought to be due to the amount of air-bearing surface to the disk. On a smoother disk, the surface is larger. So under air-bearing pressure, the slider can be lifted higher.

On the rougher disk, the AE signal is higher. This is consistent with the spacing results. On the rougher disk, the pitch angle is lower and the probability of the slider making random contact with the peaks of the disk is greater.

All three slider show higher acoustic emission as the relative velocity increased. This behavior was also observed and reported by Blanco et al. [11]. It is caused not by head disk contacts, but the closeness between HGA structural and air bearing resonant frequencies.

6 Acknowledgments

This research project is supported by the Computer Mechanics Laboratory at the University of California at Berkeley.

7. References

[1] Donovan, M. J. and Bogy, D. B., “Experimental study of Head-Disk Interface Dynamics Under the condition of Near-Contact Recording for Magnetic Disk Drive,” Doctoral Dissertation, University of California, Berkeley, CA, May 1995.

[2] Bedoy, C. and Bogy, D. B., “Effects of Disk Surface Roughness on the Flying Characteristics of Quasi-Contact Sliders,’ Technical Report 96-005 (Blue Series), Computer Mechanics Laboratory, University of California, Berkeley, CA, February 1996.

[3] Bair, C. and Bogy,¸ “Experimental study of Disk waviness effects on Proximity Air Bearing Sliders,” Master Project Report, Computer Mechanics Laboratory, University of California, CA, December 1996.

[4]Suzuki, S. and Nishihira, H., “Study of slider Dynamics over Very Smooth Magnetic Disk,” 1995 STLE/ASME Tribology Conference Excepts, Paper No. 95-Trib-38.

[5] Phase Metrics Corporation, Dynamics Flying Height Tester Operational Manual, Part No. 30, 150 Rev. D., Phase Metrics Corporation, San Diego, CA November 1994.

[6] Zygo Corporation, New View 100 Operations Manual, Part NO. OMP-0348E, Zygo Corporation, Middlefield, CT, September 1994.

[7] Acoustic Emission Technology Corporation, Operating and Instruction Manual for the AET Model 204B and 204G, Acoustic Emission Technology Cooperation, Sacramento, CA, January 1982

[8] Suk, M. and Bogy, D. B., "Head -Disk Interface Studies in Magnetic Disk Drive,' Doctoral Dissertation, University of California, Berkeley, CA, October 1991.

[9] Jeong, T. G. and Bogy, D. B., "Slider-Disk Interactions During Dynamic Load-Unload in Magnetic Recording Disk Drives," Doctoral Dissertation, University of California, Berkeley, CA, October 1991

[10]Staudenmann, M. and Bogy, D. B., " A Phase Demodulation for Interferometric Measurements at the Head Disk Interface," Technical Report 97-008 (Blue Series), Computer Mechanics Laboratory, University of California, Berkeley, CA, June 1997.

[11] Blanco, R. and Bogy, D. B., "Head -Disk Interface Dynamics of a Proximity Air Bearing slider with Various Disk Substrates and Flexure-Gimbal Designs,' M.S. Project Report, University of California, Berkeley, CA, October 1991.

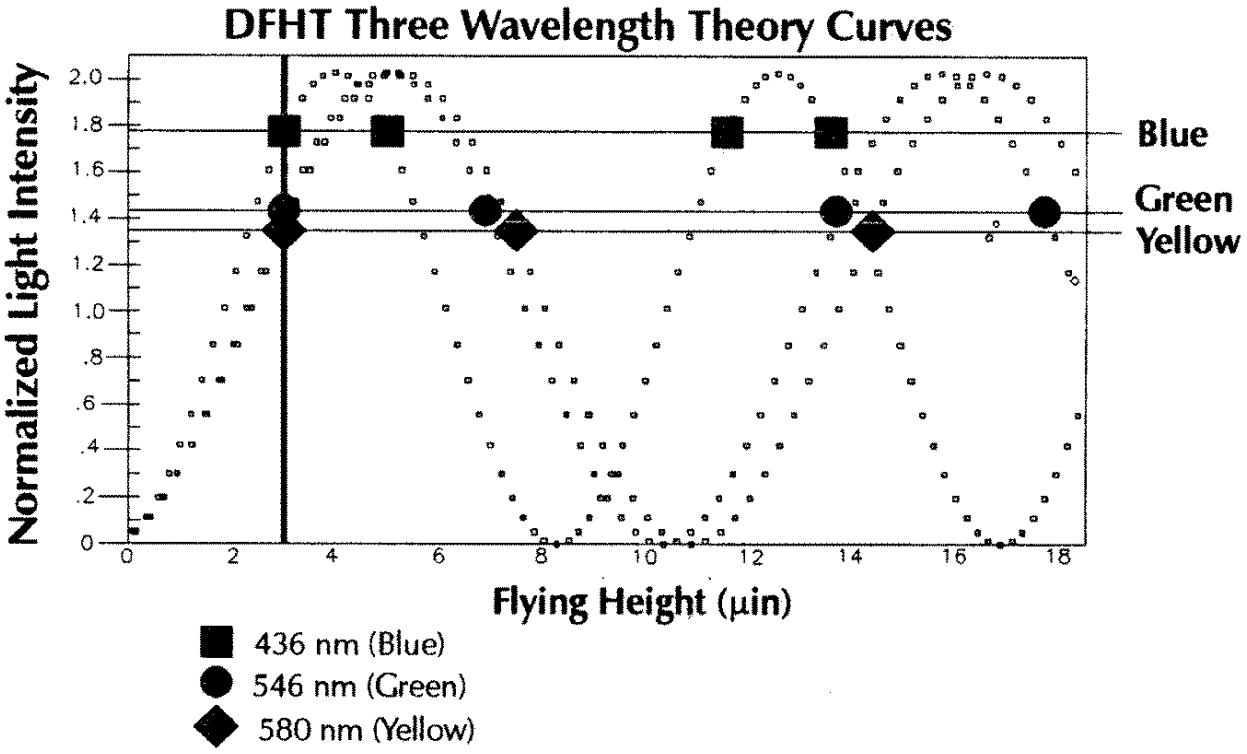

Figure 2.1 Theoretical intensity curves for interference using three wavelengths. A set of measured intensity values corresponds to a unique spacing value.

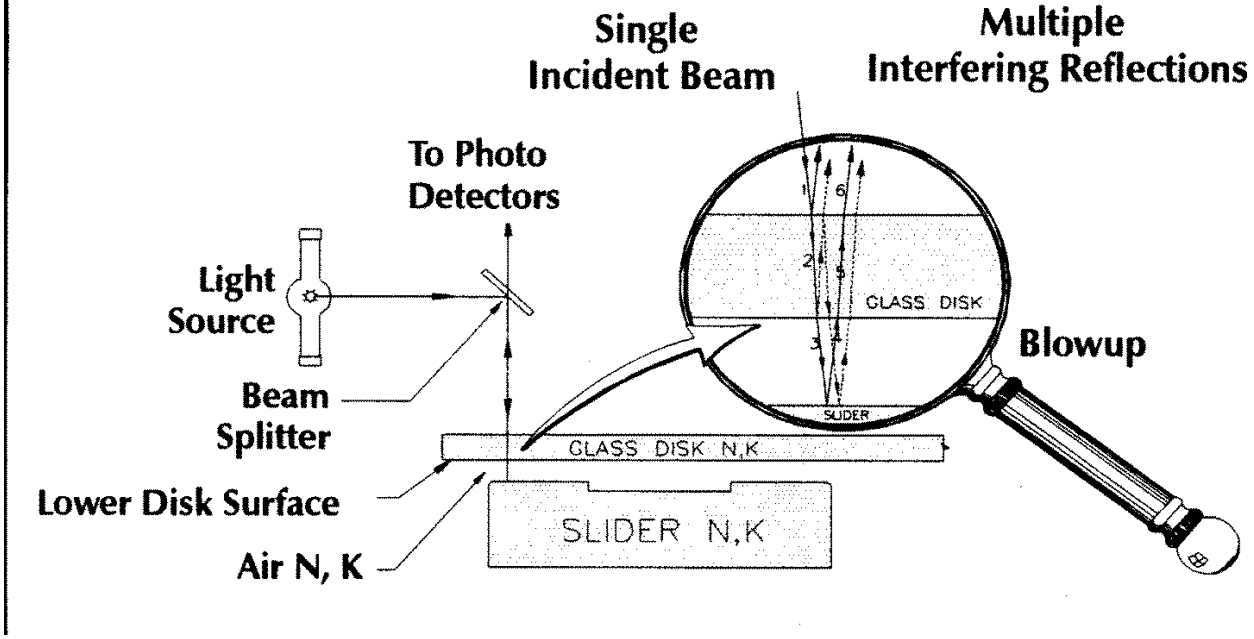

Figure 2.2 Light path in DFHT.

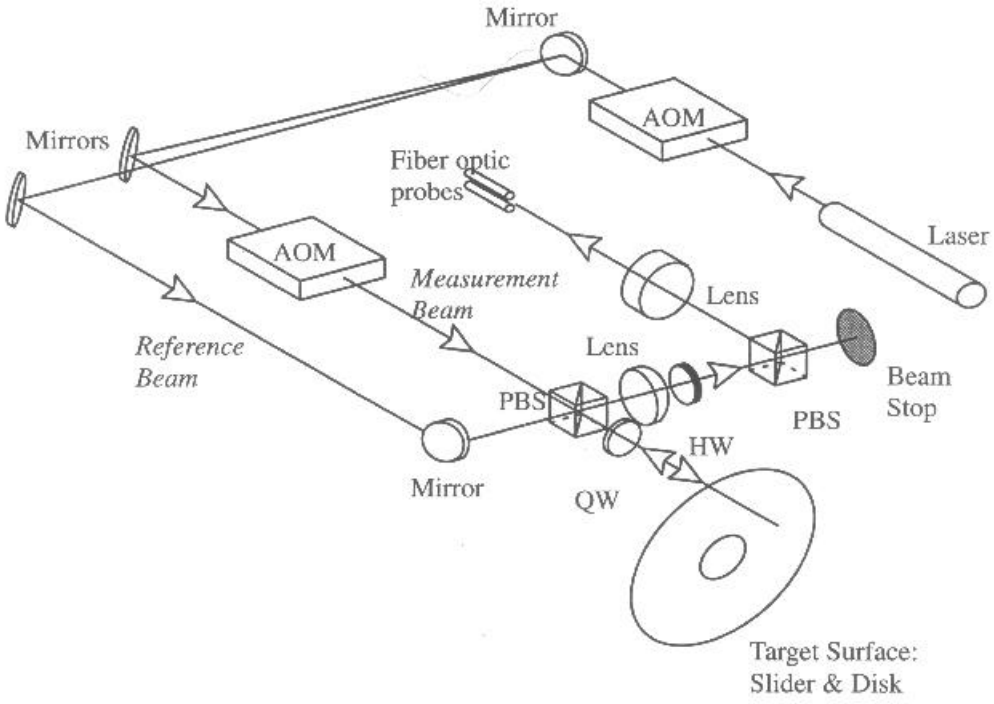

Figure 2.3 The optical layout for the Berkeley Multi-Channel Laser Interferometer.

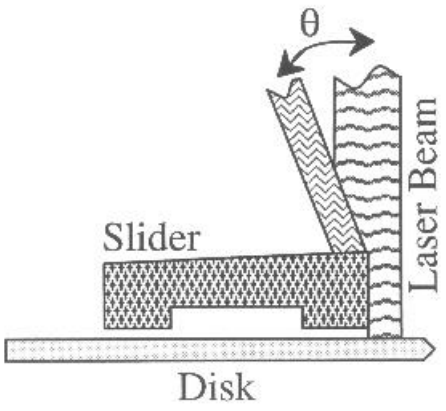

Figure 2.4 A schematic diagram showing the divergence of the reflected measurement beam when the slider's back is not parallel to the disk.

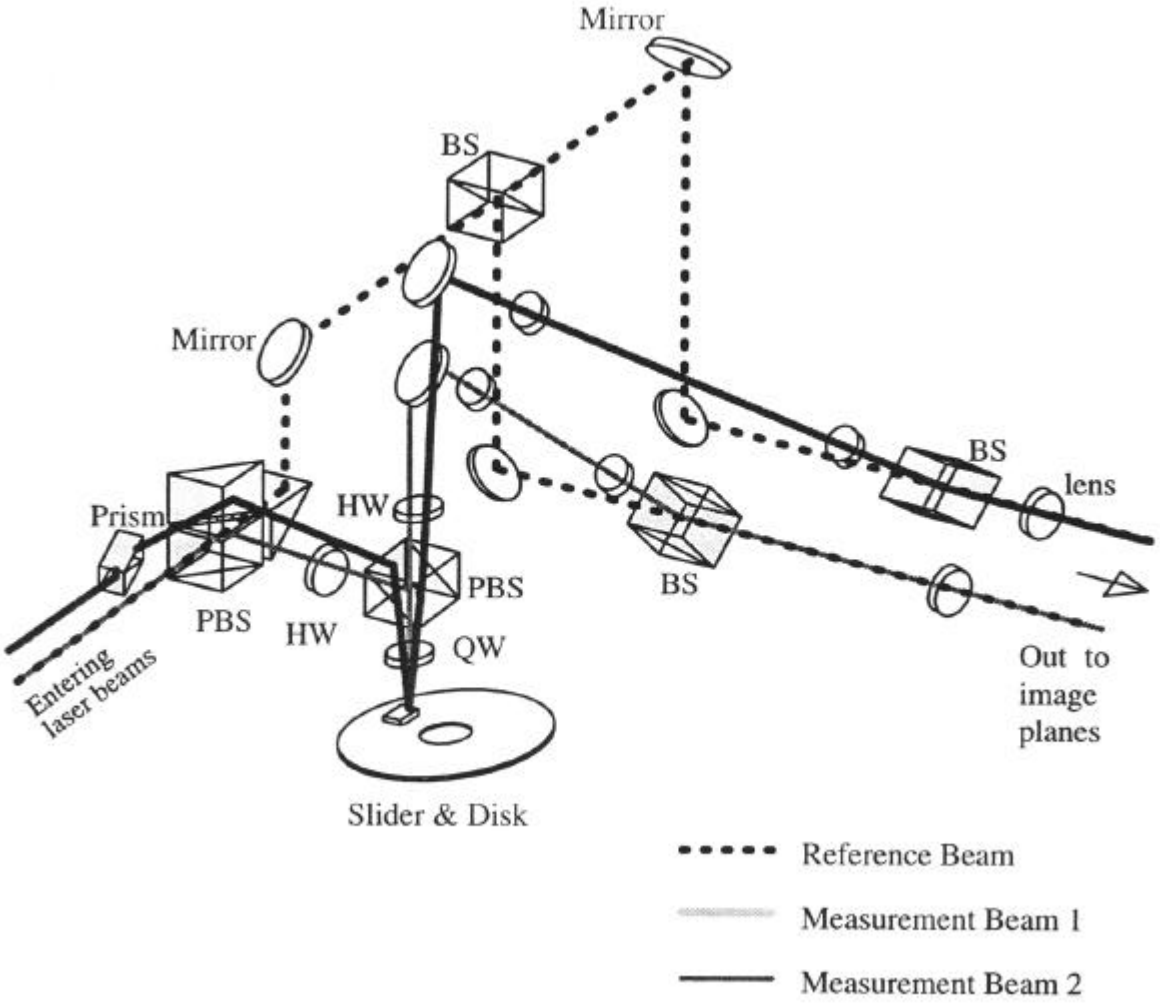

Figure 2.5 Optics configuration for the double measurement beams interferometer

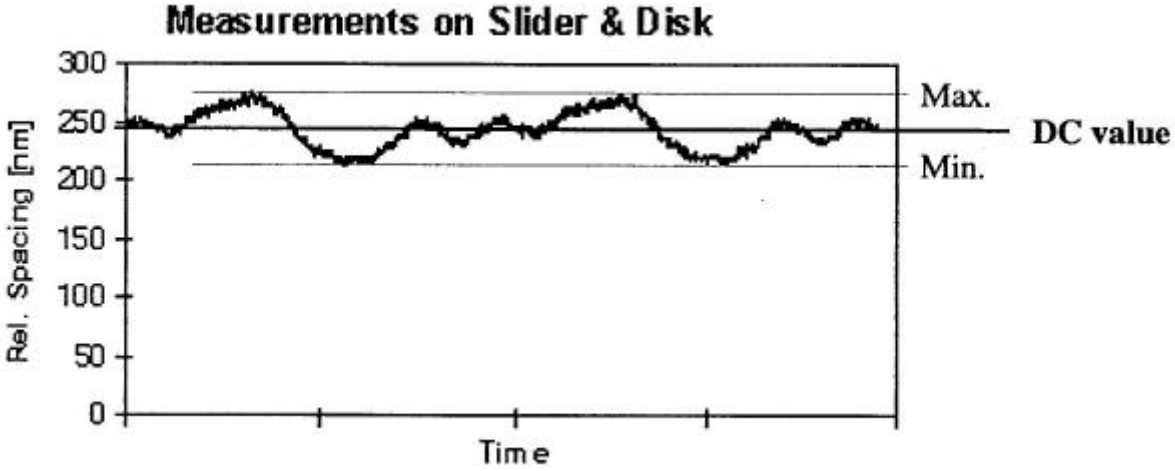

Figure 2.6 Determination of a data value in the landing curv

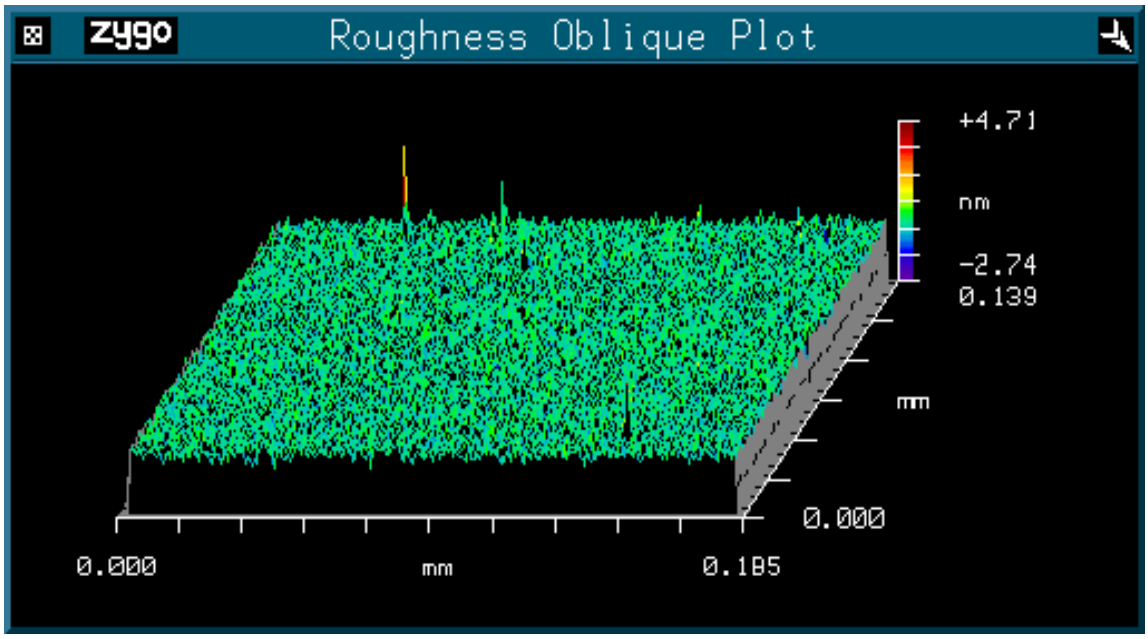

Figure 4.1 Roughness of 5 Angstrom disk

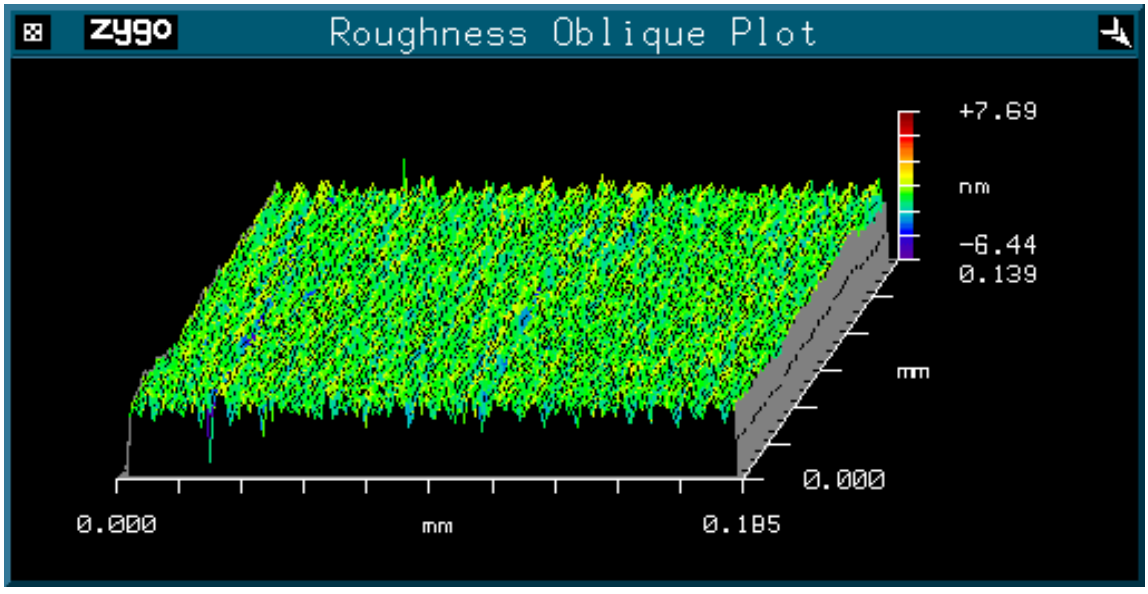

Figure 4.2 Roughness of 10 Angstrom disk

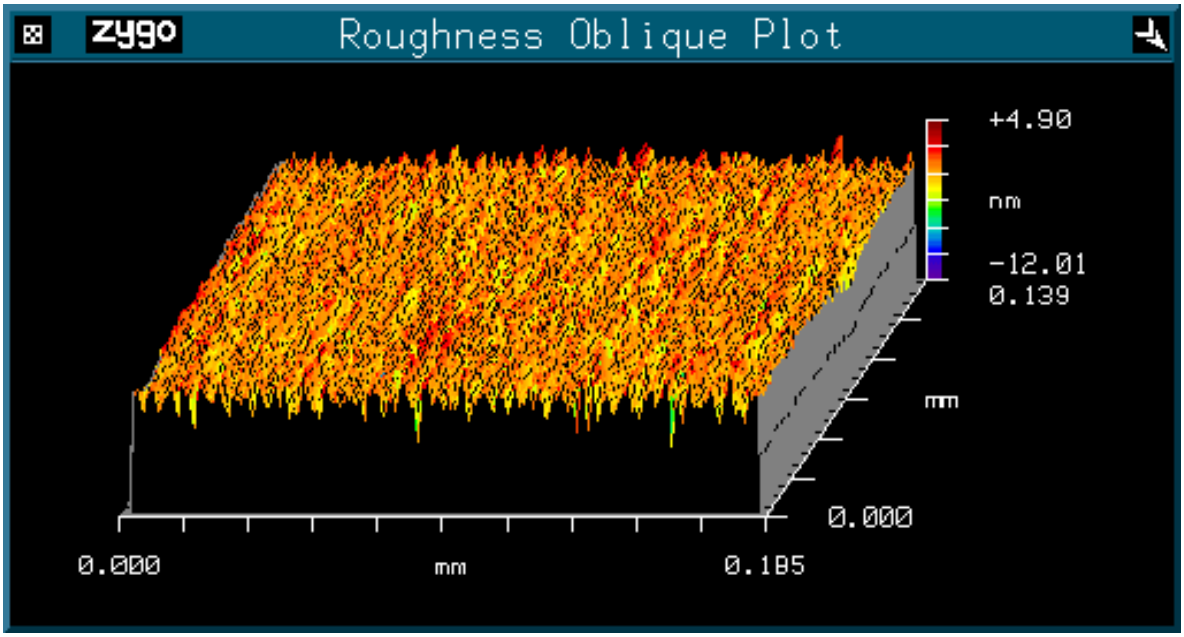

Figure 4.3 Roughness of 5 Angstrom disk

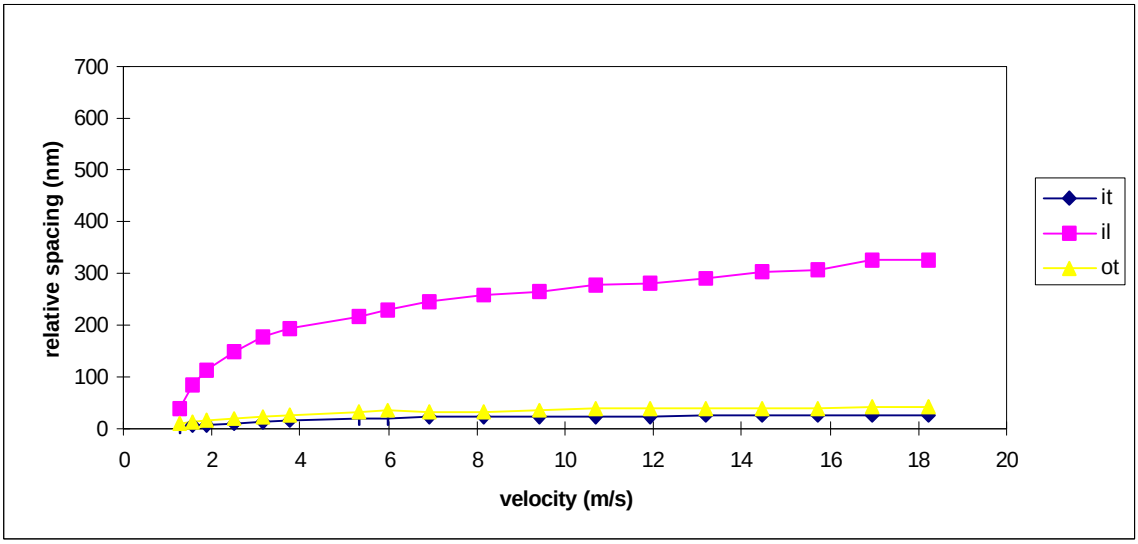

Figure 4.4 Landing curves of the AAB slider flying on the 15 Angstrom disk

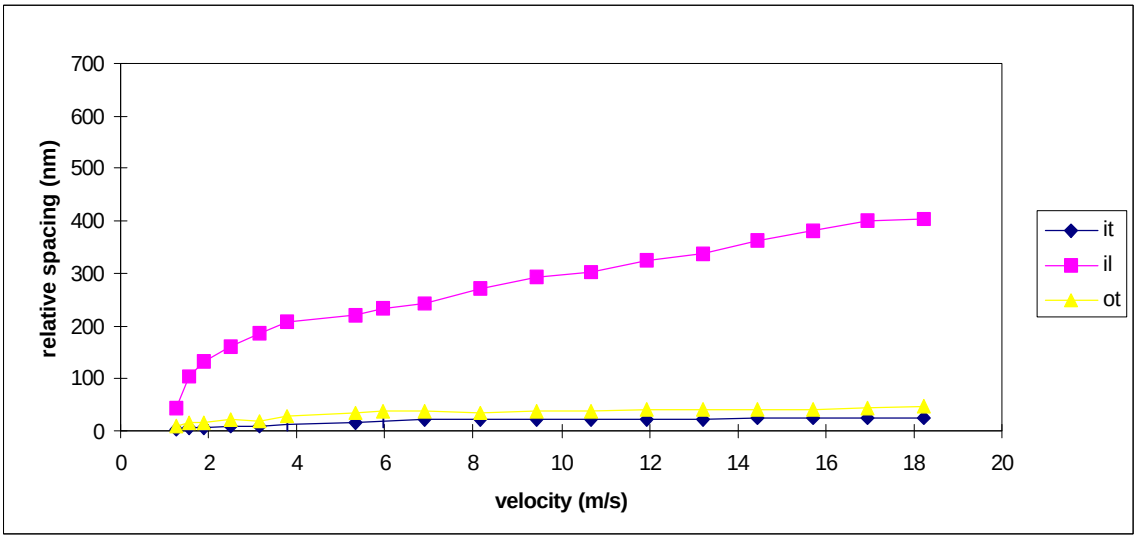

Figure 4.5 Landing curves of the AAB slider flying on the 10 Angstrom disk

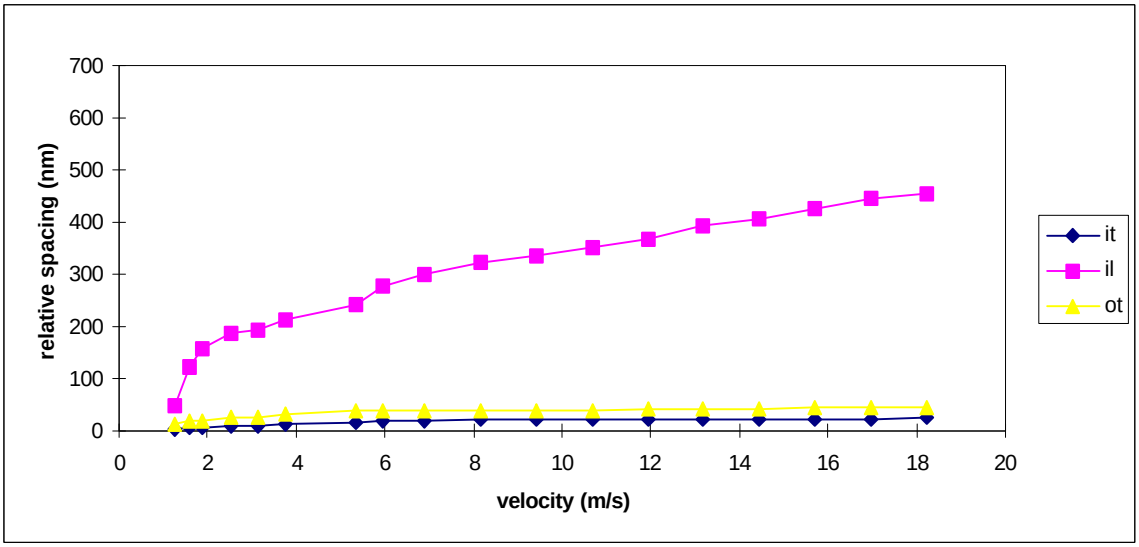

Figure 4.6 Landing curves of the AAB slider flying on the 5 Angstrom disk

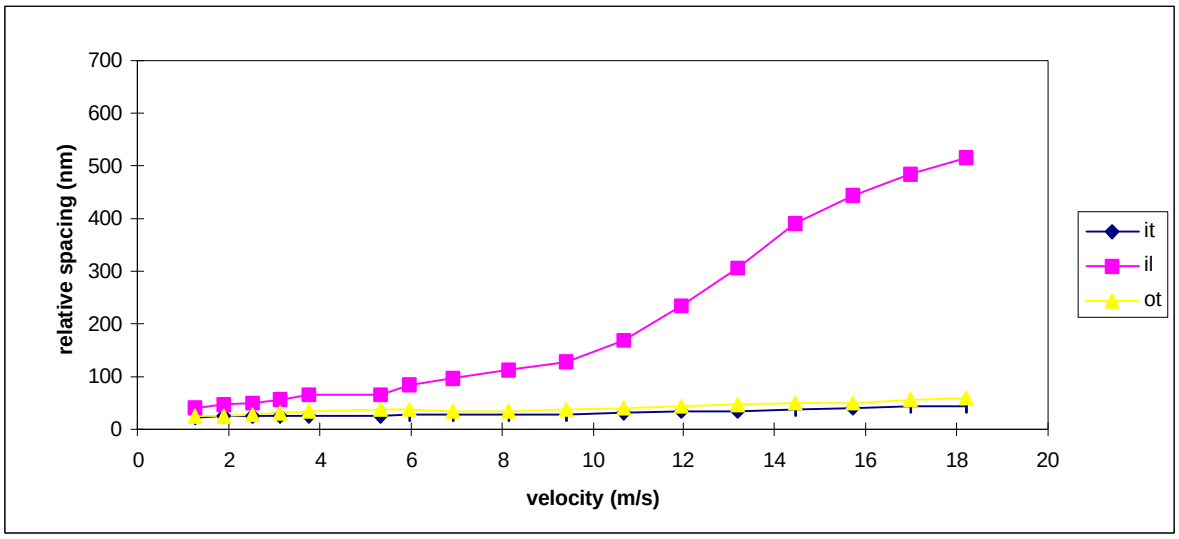

Figure 4.7 Landing curves of the Nutcracker slider flying on the 15 Angstrom disk

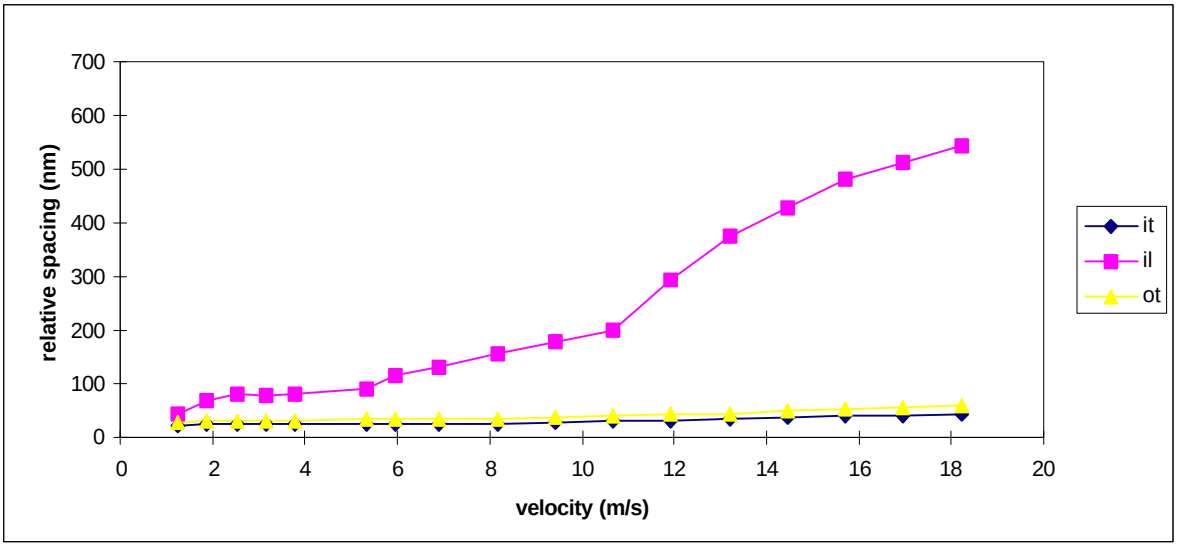

Figure 4.8 Landing curves of the Nutcracker slider flying on the 10 Angstrom disk

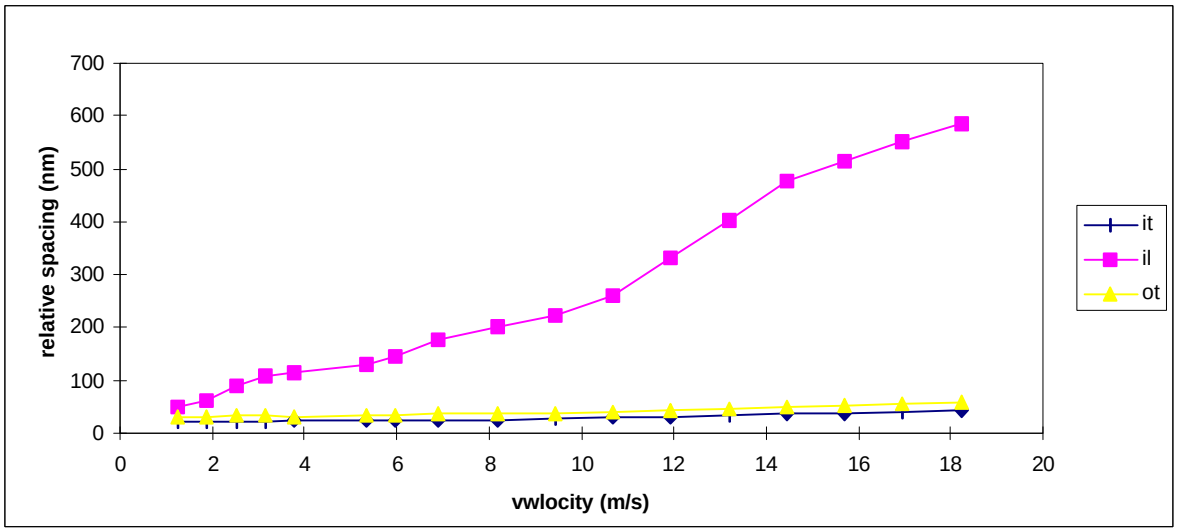

Figure 4.9 Landing curves of the Nutcracker slider flying on the 5 Angstrom disk

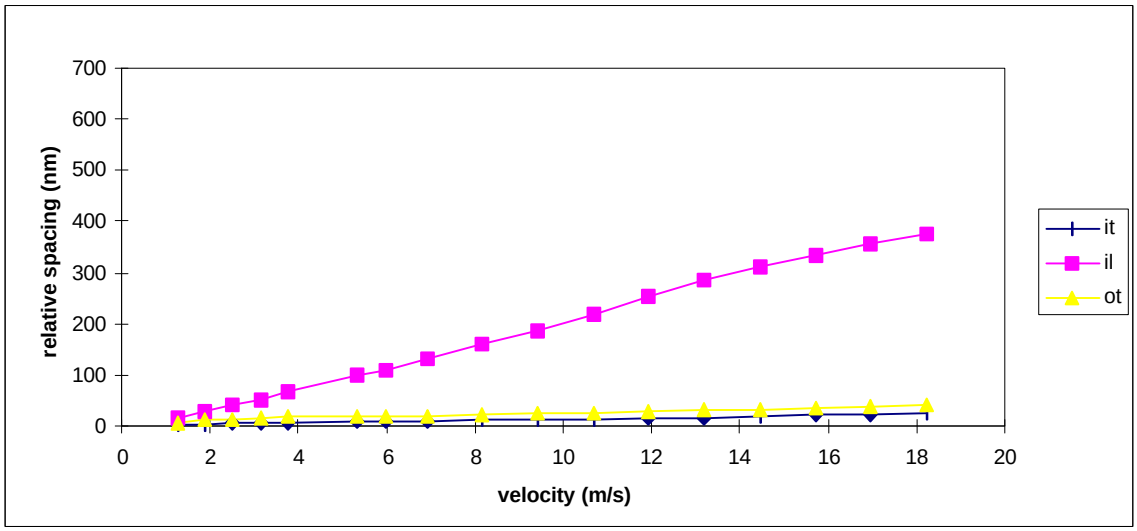

Figure 4.10 Landing curves of the Tripad slider flying on the 15 Angstrom disk

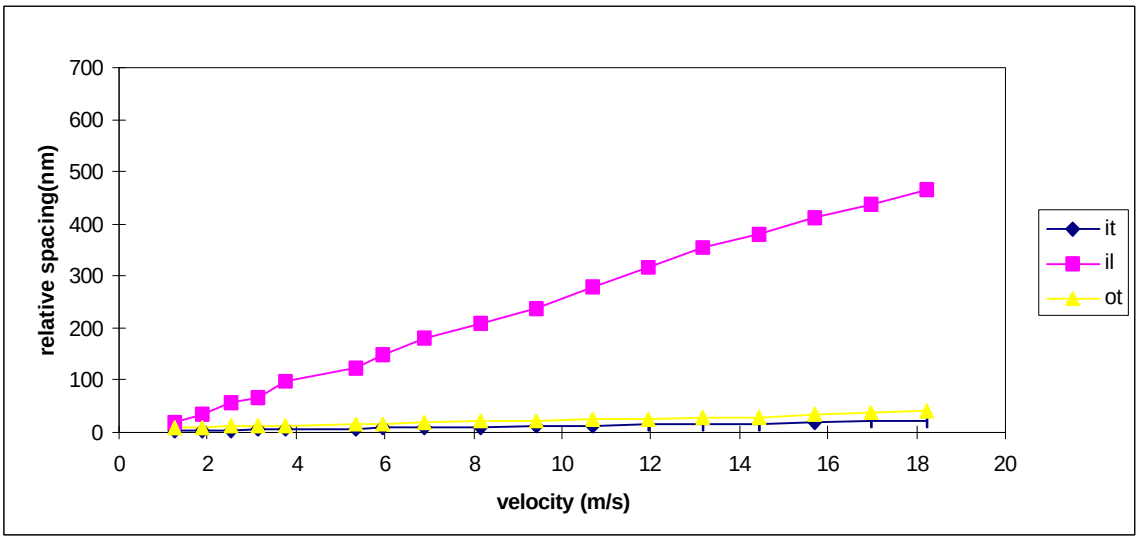

Figure 4.11 Landing curves of the Tripad slider flying on the 10 Angstrom disk

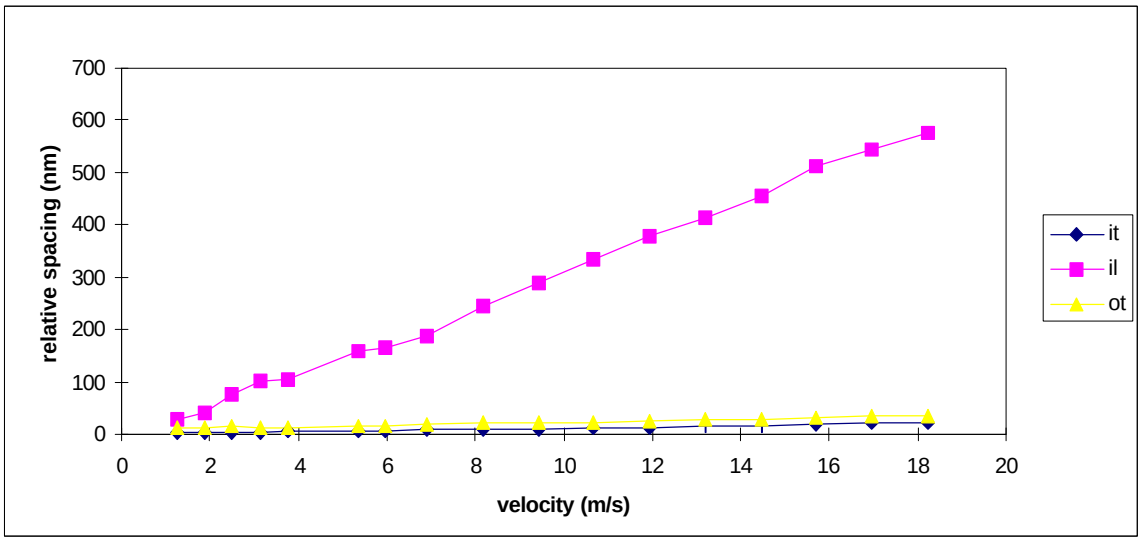

Figure 4.12 Landing curves of the Tipad slider flying on the 5 Angstrom disk

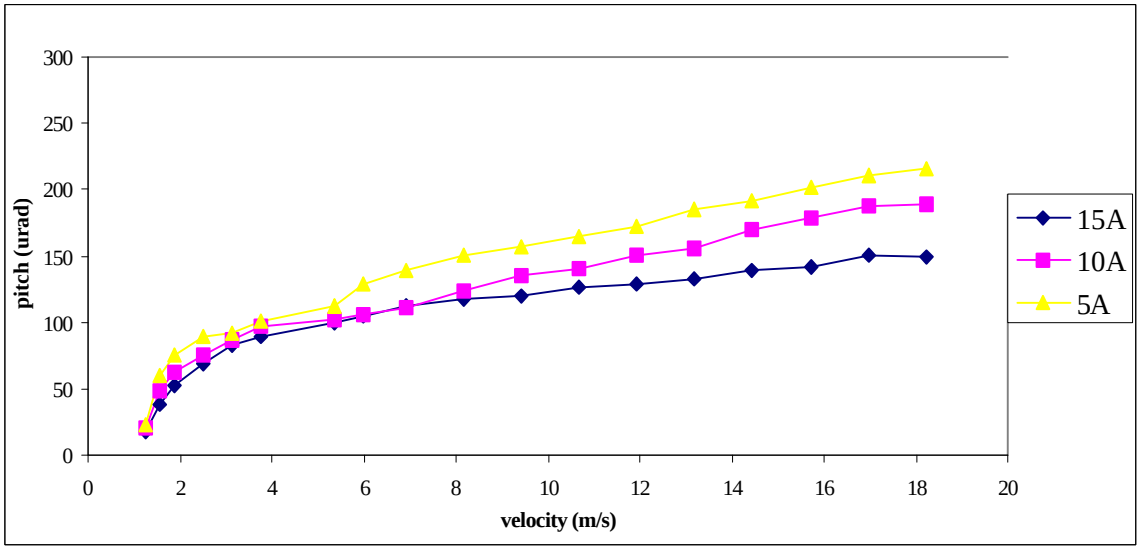

Figure 4.13 Pitch angles of the AAB slider flying on the three disks

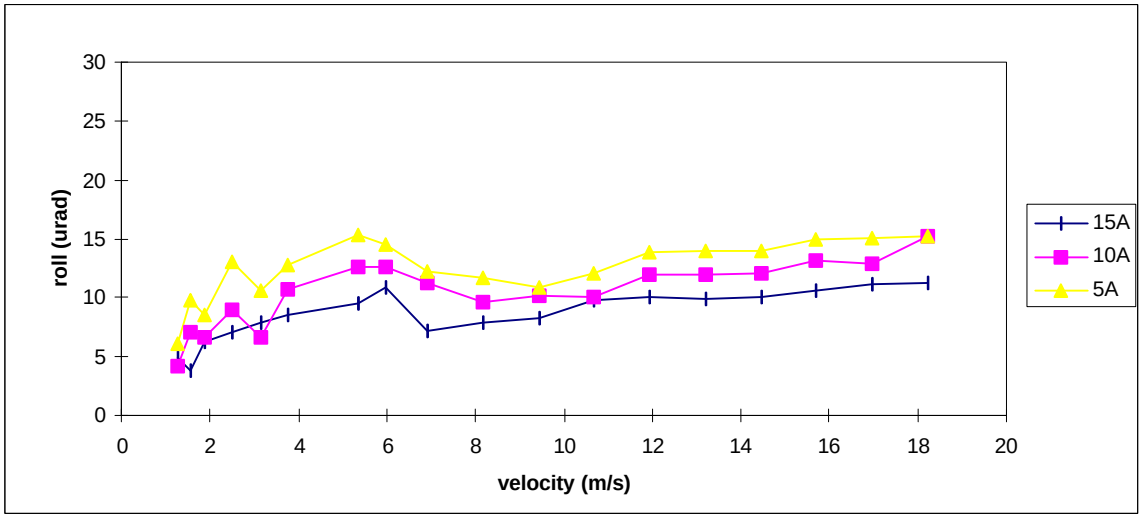

Figure 4.14 Roll angles of the AAB slider flying on the three disks

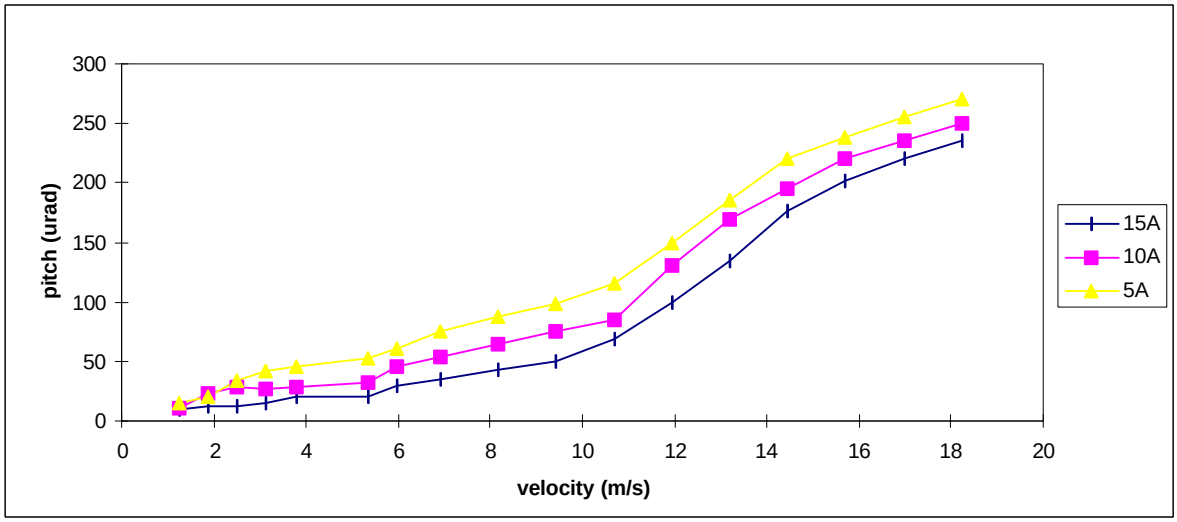

Figure 4.15 Pitch angles of the Nutcracker slider flying on the three disks

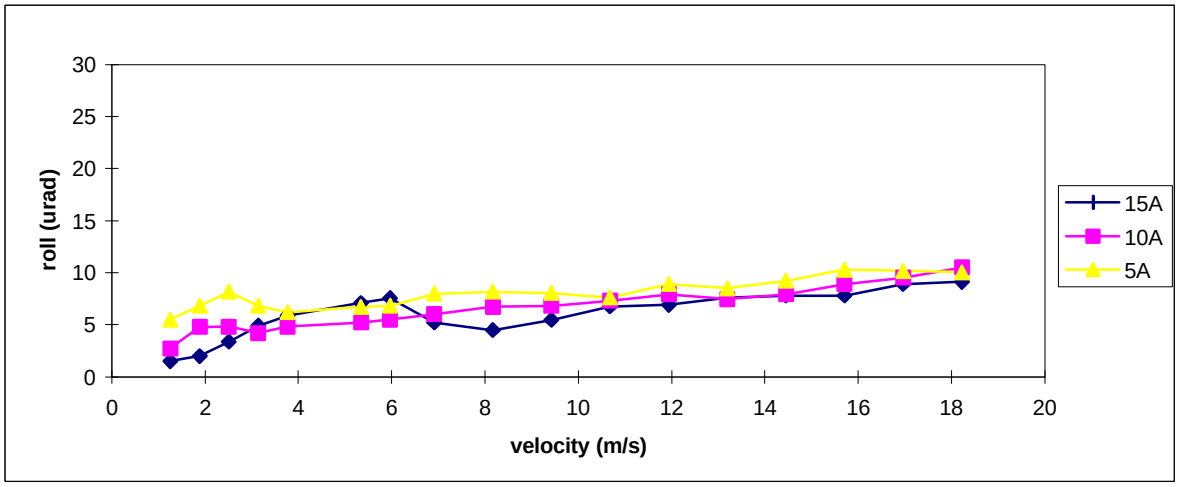

Figure 4.16 Roll angles of the Nutcracker slider flying on the three disks

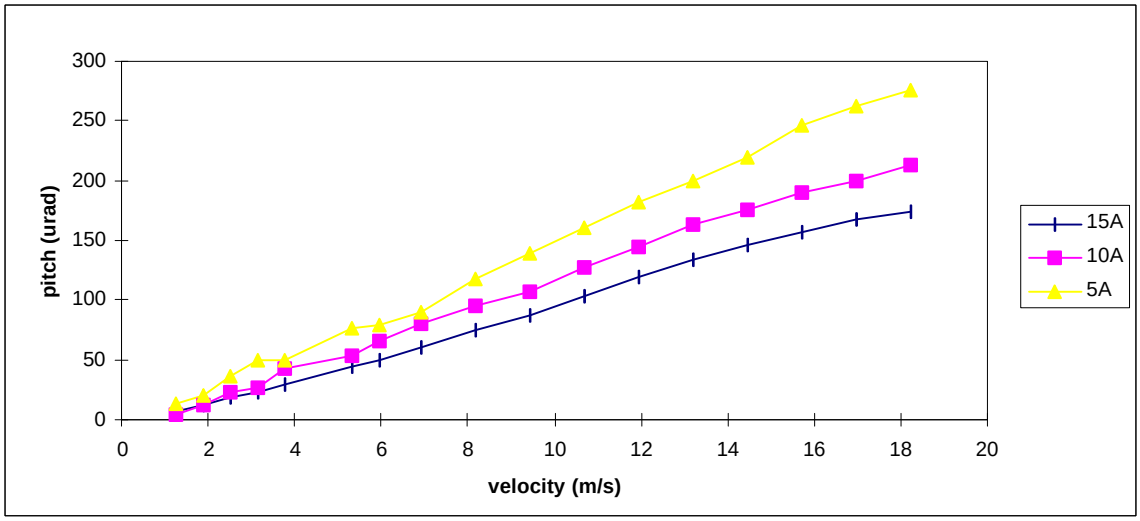

Figure 4.17 Pitch angles of the Tripad slider flying on the three disks

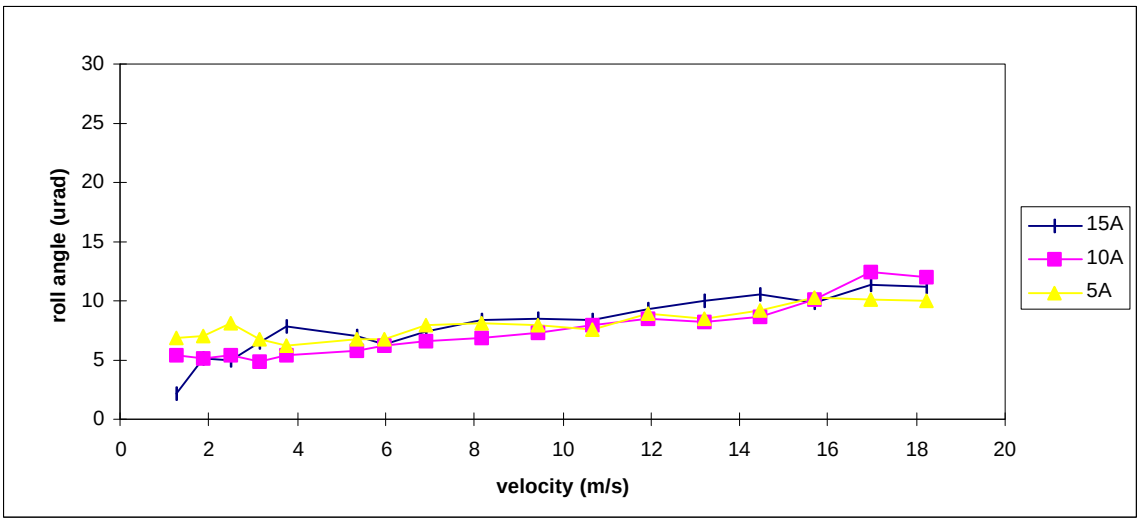

Figure 4.18 Roll angles of the Tripad slider flying on the three disks

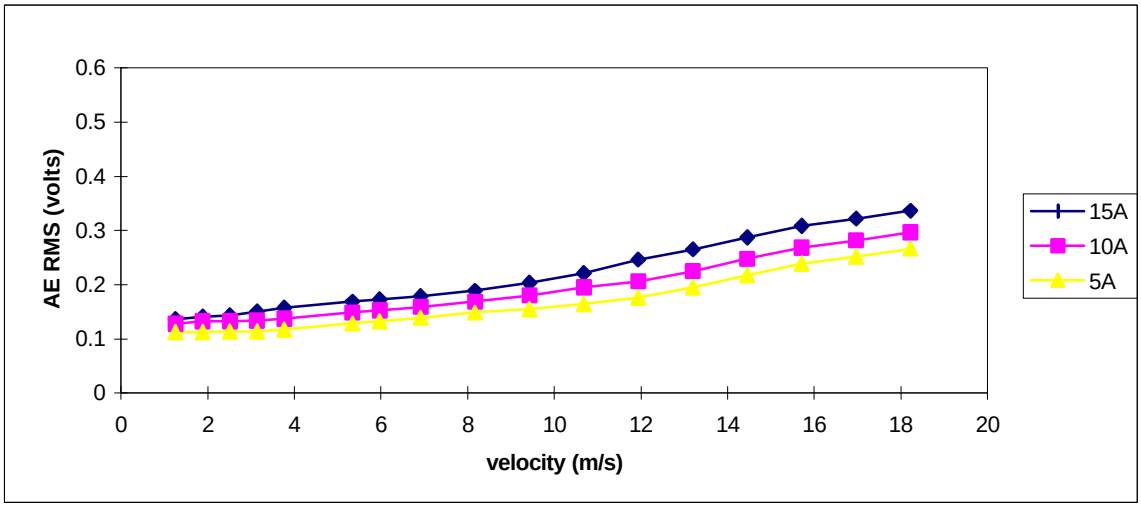

Figure 4.19 AAB slider glide avalanche on the three disks

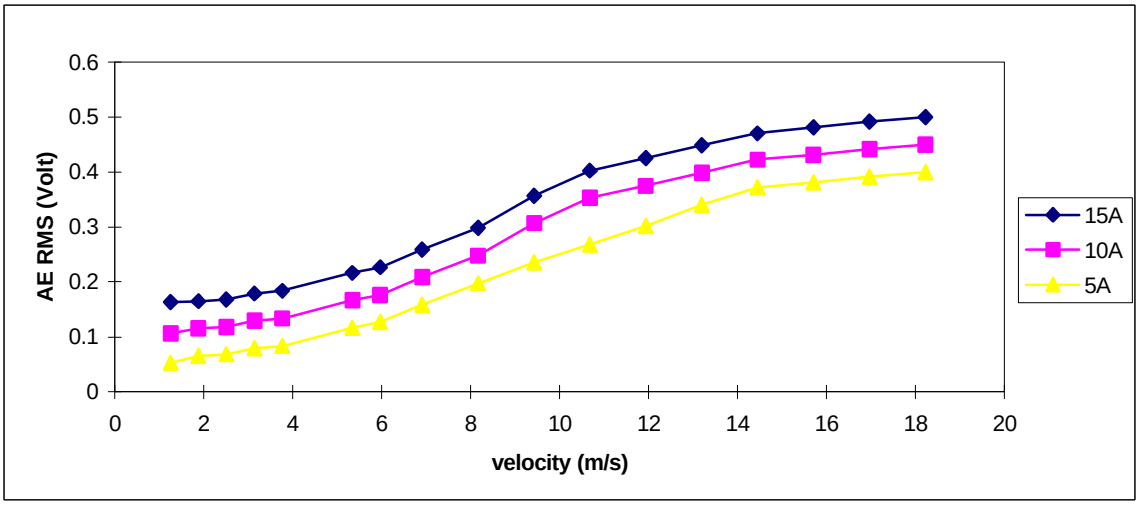

Figure 4.20 Nutcracker slider glide avalanche on the three disks

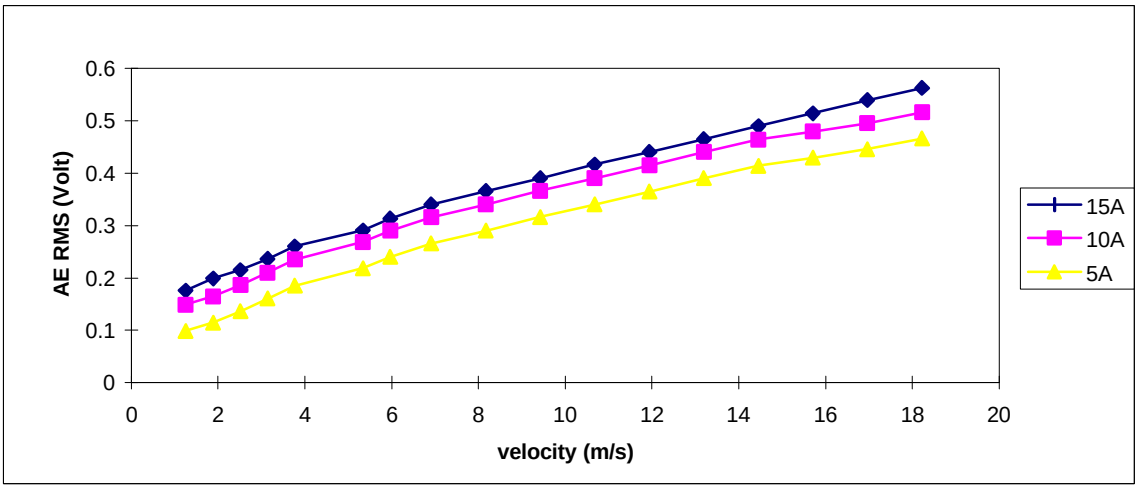

Figure 4.21 Tripad slider glide avalanche on the three disks